ISSN: 0067-2904

Monitoring the Expansion of Unplanned Urbanization and its Impact on Climate Change based on Google Earth Engine Service, a Case Study of Baghdad / Iraq

Noor Waleed *, Maythm AL-Bakri
Department of Surveying, College of Engineering, University of Baghdad, Baghdad, Iraq

Received: 28/6/2022 Accepted: 25/12/2022 Published: 29/2/2024

Abstract

The earth's surface comprises different kinds of land cover, water resources, and soil, which create environmental factors for varied animals, plants, and humans. Knowing the significant effects of land cover is crucial for long-term development, climate change modeling, and preserving ecosystems. In this research, the Google Earth Engine platform and freely available Landsat imagery were used to investigate the impact of the expansion and degradation in urbanized areas, watersheds, and vegetative cover on the land surface temperature in Baghdad from 2004 to 2021. Land cover indices such as the Normalized Difference Vegetation Index, Normalized Difference Water Index, and Normalized Difference Built-up Index (NDVI, NDWI, and NDBI) were determined to examine the effects of land cover changes. In addition, the land surface temperature was calculated to assess urbanization expansion's impact on Baghdad's climate warming. The results showed a drastic decrease in vegetative cover and green land, on the other hand, a significant expansion in urbanized areas. Hence, from 2004 to 2021, the urbanized areas and open land rose by 37% and 3%, respectively, while the vegetative cover decreased by 41%. The maximum land surface temperature has risen 4° C, and the minimum land surface temperature has risen 2.5°C.

Keywords: GEE, *LST, NDBI, NDVI, and NDWI*

مراقبة التوسع العمراني الغير مخطط له و تأثيره على تغيير المناخ بالاعتماد على خدمة محرك كوكل ايرث، بغداد/ العراق كمنطقة دراسة

نور وليد يونس*, ميثم مطشر البكري
قسم المساحة, كلية الهندسة, جامعة بغداد, محافظة بغداد, العراق

الخلاصة

يتكون سطح الأرض من أنواع مختلفة من الغطاء الأرضي ، والموارد المائية ، والتربة ، مما يخلق عوامل بيئية للحيوانات والنباتات المتنوعة وكذلك البشر. إن معرفة التأثيرات الكبيرة للغطاء الأرضي أمر بالغ الأهمية للتنمية طويلة الأجل، ونمذجة تغير المناخ، والحفاظ على النظم البيئية. في هذا البحث، تم استخدام منصة Google Earth Engine جنبًا إلى جنب مع صور لاندسات المتاحة مجانًا للتحقيق في تأثير التوسع والتدهور لكل من المناطق الحضرية ومستجمعات المياه والغطاء النباتي على درجة حرارة سطح الأرض في بغداد من 2004 إلى 2021. استخدمت مؤشرات الغطاء الأرضي مثل NDVI و NDWI و NDBI لفحص تأثيرات

*Email: noor.younus1512m@coeng.uobaghdad.edu.iq

تغيرات الغطاء الأرضي. بالإضافة إلى ذلك ، تم حساب درجة حرارة سطح الأرض لتقييم تأثير التوسع الحضري على الاحتباس الحراري في بغداد. أظهرت النتائج النهائية حدوث انخفاض حاد في الغطاء النباتي والأراضي الخضراء، من ناحية أخرى، توسع كبير في المناطق العمرانية. ومن عام 2004 إلى عام 2021، ارتفعت المناطق الحضرية والأراضي المفتوحة بنسبة 37٪، و 3٪ على التوالي، بينما انخفض الغطاء النباتي بنسبة 41٪. ارتفعت درجة حرارة سطح الأرض العظمى بمقدار 4 درجات مئوية، وارتفعت درجة حرارة سطح الأرض الصغرى بمقدار 2.5 درجة مئوية.

1. Introduction

Recurring land cover/ use change (LULC) has an ever-worsening negative influence on a variety of facets of the Earth's surface, including climatic changes, biodiversity, hydrological cycle, and terrestrial ecosystems [1] [2]. (Jasim & Kamel, 2017) [3] stated that the green cover and exterior landscape are essential at the University of Baghdad campus for achieving comfort and encouraging social interactions among students. The outcomes demonstrated that walking, comfort, and relaxation were the most significant. Natural shading from plants is also preferred over artificial shading. Thus, the knowledge of land cover is essential in many spheres of life, including politics, economics, and science. Because exact land cover data determines the precision of all subsequent applications, precise and up-to-date data is in high demand [4]. Rural-urban migration has expanded significantly due to urbanization expansion's greater accessibility in amenities, employment, and production. Urbanization became a significant socioeconomic issue affecting LU change globally[5].

Urbanization is the process of converting green lands for human usage. For instance, Baghdad has seen an increase in urbanization due to recent economic expansion and overpopulation. This conversion significantly impacts climate because buildings and road cover absorb significant solar radiation rates during the day and at night. Evaporation rates rose as urbanization increased and vegetation degradation fell. These factors suggest that inadequate land use planning harms the regional climate [6]. Urbanization also affects water quality, and more recent attention has focused on this issue; for example, [7] assessed the water quality of the Tigris River by measuring the river's physicochemical parameters in Baghdad, Iraq, from Feb. 2017 to Feb. 2018. Four locations were chosen from upreach, reach, and down reach (Al-Sarrafia Bridge, Al-Shuhada Bridge, Al-Muthanna Bridge, and Al-Dora Bridge). The air temperature, water pH, electrical conductivity, salinity, and water flow were calculated in the field. All parameters varied in both seasons, according to the findings (wet and dry). This indicates that the Tigris River in the heart of Baghdad is becoming more polluted due to anthropogenic influences.

Recent investigators have also examined the effects of urbanization on the variation of LU/LC. For instance, using remote sensing and GIS software, [8] analyzed three historical LU/LC maps for Baghdad from 1985 to 2000 and 2000 to 2020. The findings revealed that urban construction land overgrows, while farmland and vegetation cover lost significant coverage over the last 35 years. (Fahad et al., 2020) [9] studied and explored Baghdad's land use and land cover variation over 28 years from 1990 to 2018. Baghdad Landsat TM and OLI 8 images were obtained from the USGS website. The images were classified into five cover classes using supervised classification: urban area, water bodies, vegetative area, barren land, and wetland, using ENVI and ArcGIS software. The accuracy was 85.11% and 88.14%, respectively. According to the change detection analysis, urban area and soil land levels have increased by 3% and 20%, respectively, while vegetation, wetlands, and water bodies have declined by 5%, 17%, and 1%, respectively.

Recently, Google Earth Engine (GEE) has been used to investigate the urbanization process. It is an online platform with science-based algorithms and processing capacity, which can be used to analyze the temporal and spatial changes in urban areas based on satellite imagery [10]. Several literature studies have adopted this platform; for example, [10] analyzed the urbanization process for Mawlamyine city using the Google Earth Engine platform for temporally and spatial urbanization areas analysis, derived from Landsat 5, 8, and (TOA) imagery. The primary goal was to assess the derived values which can be employed to assess urban areas using Google Earth Engine (GEE). The analysis yields high-quality vegetation, water, and built-up values. [11] identified different types and distributions of land cover in the southeastern United States using Google Earth Engine (GEE). Geospatial technology, NAIP high-resolution imagery, and imagery from the Landsat, SPOT, and National Agriculture Imagery Program (NAIP) were used to investigate the land use changes in urbanizing areas. All vegetation indices, such as NDVI, EVI, GRVI, MSAVI, and NDWI, were calculated for every image for 2013, 2015, and 2017. The results revealed that the barren land area increased significantly from 2013 to 2015 and declined in 2017.

This study set out to investigate the use of the Google Earth Engine platform to compute the expansion of urbanized areas and the degradation of vegetative areas in Baghdad city from 2004 to 2021. The fluctuation of watersheds using land cover indices and their impacts on land surface temperature rise were also determined and analyzed.

2. Study area and Datasets

Baghdad city, the capital of Iraq, was chosen as a study area, located in the middle of the country between 32° 48′00″ N-33°46′00″ N latitude and 43°51′00″ E-44° 56′00″ E Longitude, with an area of 5095.0 km^2 in 2021, Figure 1. Baghdad has a semi-desert climate, hot and dry in summer, with some dust storms, and cold and rainy sometimes in winter. The study area was subjected to many changes in land cover, land uses, and average temperatures, in addition to changes in the area and shape of the administrative borders during 2004-2021. Urban construction-related land expansion, inhabitance growth, and evolution of socioeconomic issues affect land uses. Thus, it is crucial to assess the effects of urban sprawl and its accelerated LU/LC and understand them to direct land surface resources for sustainable development.

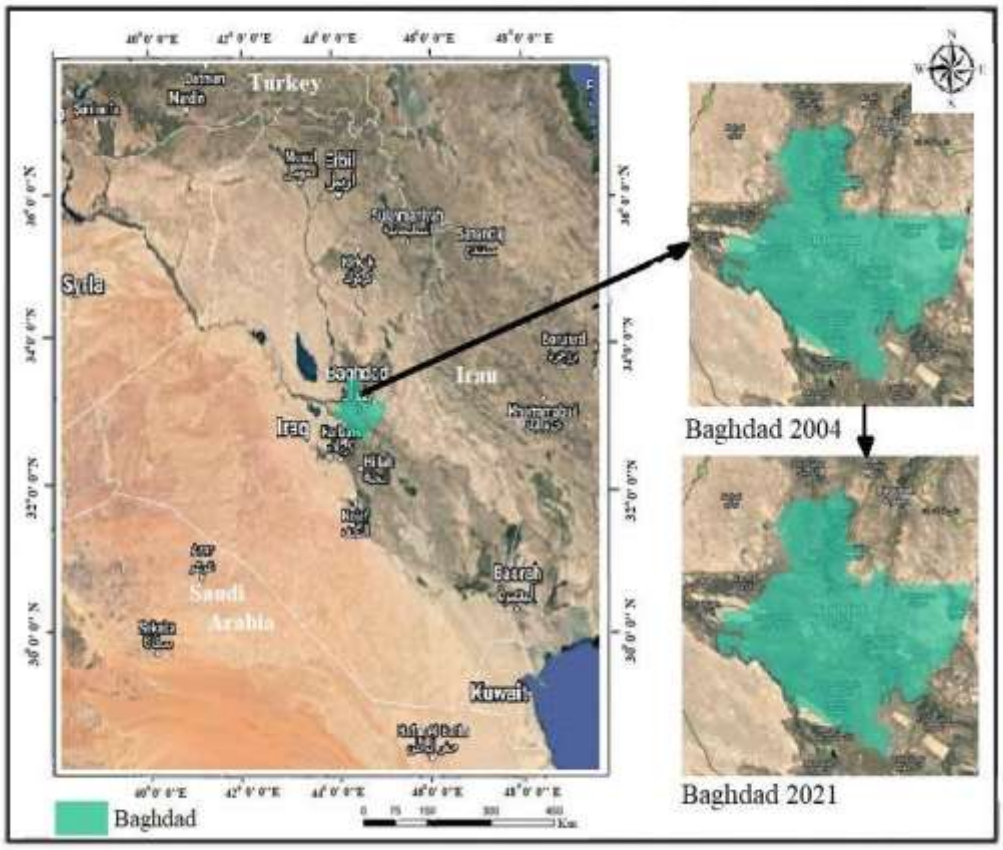

Figure 1: The study area during the study period.

3. Method and Materials

The Google Earth Engine (GEE) is a digital geospatial remote sensing, and it offers access to software and algorithms for processing data without participating in auxiliary data and using existing products. Global time-series aerial photographs and vector data are also accessible through the Code Editor Application Program Interface (API) on the web [12]. A set of satellite images from Landsat (TM) and (OLI) images, which GEE offers, were utilized to extract the indices areas and land surface temperature for Baghdad over the study period, July (2004, 2008, 2013, 2017, and 2021). The collected images were filtered as a zero-cloud collection.

3.1. processing of the data

The first step started by creating a folder for the study area using Java scripts via the Application Programming Interfaces (API) of GEE. Baghdad vector data, which the General Authority delivers for Survey in Iraq, was uploaded from (Scripts) in Code Editor to filter data according to the geometry of the area of interest. Then select the images (Landsat5 and 8) and filter them by date and cloud cover. According to the vector data, Baghdad is covered with two satellite images, which must be merged to execute it, then write the code of (centerObject) to put the vector map layer in the center of the API screen. Finally, these statements must be printed in the API command to see the vector data and the satellite imagery that is chosen as an output. Then (Run) can be clicked to appear the result in (The console and Layer manager) after running the Java scripts commend, Figure 2.

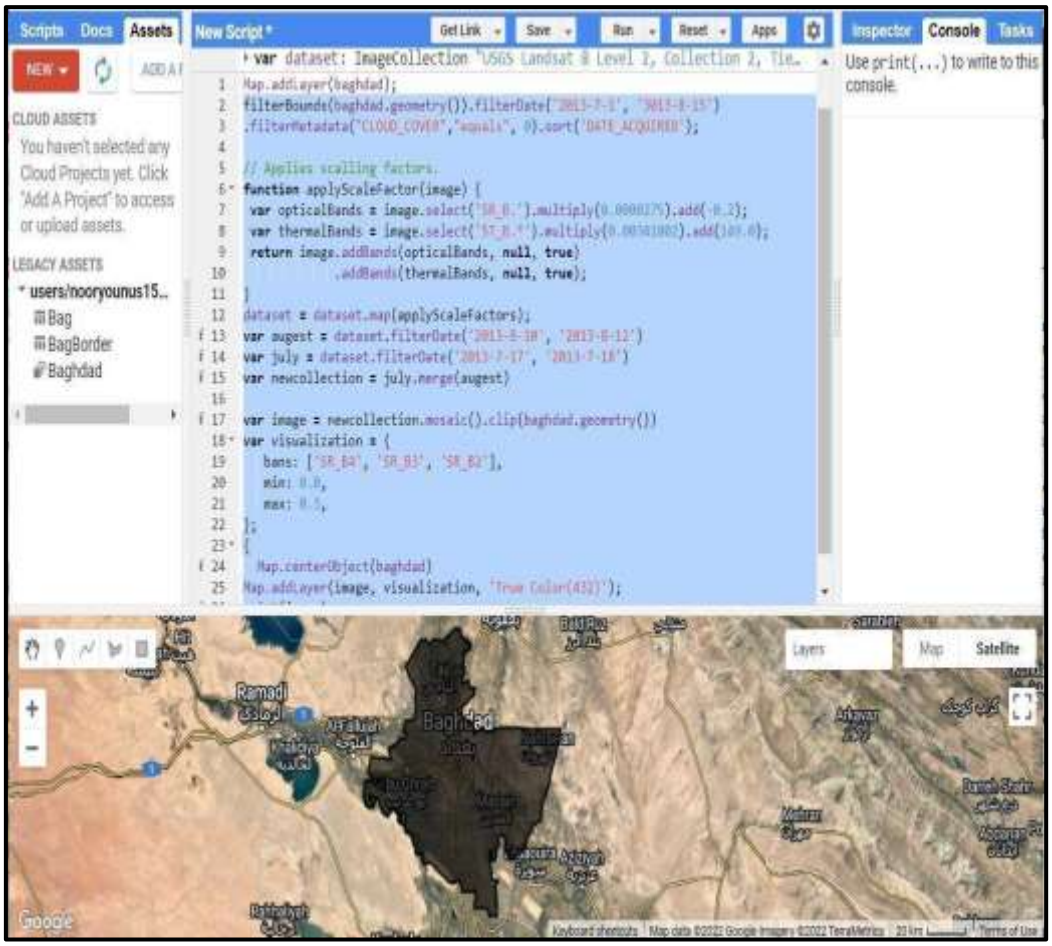

Figure 2: Uploading vector data and Landsat imagery and filtering on API.

This study employed two multispectral satellite imageries: Landsat (TM) imagery for 2004 and 2008 and Landsat (OLI) Top of Atmosphere (TOA) imagery for 2013, 2017, and 2021 over Baghdad City. These images were primarily used to analyze the city's urban expansion and the decline of greenery land. Landsat images were resampled to 30m resolution. All the reflective bands, except the thermal band, were used in classification tasks. The GEE displays data as a true color for Landsat 5 (B3, B2, and B1) and Landsat 8 (B5, B4, and B2). It also can display false color, which benefits land cover extraction.

3.2. NDVI Extraction

The NDVI Index methodology was adopted to calculate the area of greenery lands in Baghdad; it consists of two spectral bands (Red and NIR), see Eq. 1. The results would be between (-1 to +1); the positive is the green areas and vegetative coverage, while the negative values are neglected [13]. Figure 3 presents the GEE code written in Javascript inside the code editor. These codes were used for Landsat 5 and 8 to compute the NDVI for the study area.

$$NDVI = (NIR_{band} - Red_{band}) / (NIR_{band} + Red_{band}) \quad \text{……..(1).}$$

NDVI calculated by GEE using the code below:

```
//median (ndvi) for Landsat 8
var ndvi =
image.normalizedDifference(['SR_B5','SR_B4']).rename('NDVI');
var ndviparams = {min: -1, max: 1, palette: ['blue', 'white', 'green']};
print(ndvi, 'ndvi');
Map.addLayer(ndvi, ndviparams, 'ndvi');
}
 //median (ndvi) for Landsat 5
var ndvi =
image.normalizedDifference(['SR_B4','SR_B3']).rename('NDVI');
var ndviparams = {min: -1, max: 1, palette: ['blue', 'white', 'green']};
print(ndvi, 'ndvi');
Map.addLayer(ndvi, ndviparams, 'ndvi');
}
```

Figure 3: Shows the GEE codes for calculating the NDVI.

3.3. NDBI Extraction

The NDBI Index methodology was adopted to calculate Baghdad's built-up lands and urbanized areas. It consists of two spectral bands: the Short-Wave Infrared (SWIR) and near-infrared (NIR) bands, see Eq.2. Figure 4 presents the GEE code written in Javascript inside the code editor. The code was used for Landsat 5 and 8 to compute the NDBI for the study area.

$$NDBI = (SWIR_{band} - NIR_{band}) / (SWIR_{band} + NIR_{band}) \quad ...(2)$$

NDBI calculated by GEE using the code below:

```
//median (ndbi) for Landsat 8
var ndbi =
image.normalizedDifference(['SR_B6','SR_B5']).rename('NDBI');
var ndbiparams = {min: -1, max: 1, palette: ['blue', 'white', 'red']};
print(ndbi, 'ndbi');
Map.addLayer(ndbi, ndbiparams, 'ndbi');
}
 //median (ndbi) for Landsat 5
var ndbi =
image.normalizedDifference(['SR_B5','SR_B4']).rename('NDBI');
var ndbiparams = {min: -1, max: 1, palette: ['blue', 'white', 'red']};
print(ndbi, 'ndbi');
Map.addLayer(ndbi, ndbiparams, 'ndbi');
}
```

Figure 4: Shows the GEE code for calculating the NDBI.

3.4. NDWI Extraction

The NDWI Index methodology was adopted to calculate Baghdad's water lands and watershed areas. It consists of two spectral bands: the green and near-infrared (NIR) bands, see Eq.3. The results would be between (-1 to +1), and the positive values are the watersheds [14]. Figure 5 presents the GEE code written in Javascript inside the code editor. The code was used for Landsat 5 and 8 to compute the NDWI for the study area.

$$NDWI = (Green_{band} - NIR_{band}) / (Green_{band} + NIR_{band}) \quad \ldots\ldots\ldots(3)$$

NDWI calculated by GEE using the code below:

```
//median (ndwi) for Landsat 8
var ndwi =
image.normalizedDifference(['SR_B3','SR_B5']).rename('NDWI');
var ndwiparams = {min: -1, max: 1, palette: ['blue', 'white', 'red']};
print(ndwi, 'ndwi');
Map.addLayer(ndwi, ndwiparams, 'ndwi');
}
 //median (ndwi) for Landsat 5
var ndwi =
image.normalizedDifference(['SR_B2','SR_B4']).rename('NDWI');
var ndwiparams = {min: -1, max: 1, palette: ['blue', 'white', 'red']};
print(ndwi, 'ndwi');
Map.addLayer(ndwi, ndwiparams, 'ndwi');
}
```

Figure 5: Shows the GEE code for calculating the NDWI.

3.5. Land surface temperature calculation

The TOA and thermal bands (band 10 for Landsat8 and band 6 for Landsat 5) were utilized to calculate the land surface temperature. Figure 6 presents the GEE code, which was written in Java script inside the code editor of GEE for achieving processing and calculations.

```
Imports (1 entry)
  var baghdad: Table users/nooryounus1512m/Bag
Map.addLayer(baghdad);
var dataset = ee.ImageCollection("LANDSAT/LC08/C02/T1_L2")
.filterBounds(baghdad.geometry()).filterDate('2013-7-1','2013-8-15')
.filterMetadata("CLOUD_COVER","equals", 0).sort('DATE_ACQUIRED');
// Applies scaling factors.
function applyScaleFactors(image) {
  var opticalBands = image.select('SR_B.').multiply(0.0000275).add(-0.2);
  var thermalBands = image.select('ST_B.*').multiply(0.00341802).add(149.0);
  return image.addBands(opticalBands, null, true)
              .addBands(thermalBands, null, true);
}
dataset = dataset.map(applyScaleFactors);
var augest = dataset.filterDate('2013-8-10','2013-8-12')
var july = dataset.filterDate('2013-7-16','2013-7-18')
var newcollection = july.merge(augest)
var image = newcollection.mosaic().clip(baghdad.geometry())
var visualization = {
  bands: ['SR_B4', 'SR_B3', 'SR_B2'],
  min: 0.0,
  max: 0.3,
};
{
Map.centerObject(baghdad)
Map.addLayer(image, visualization, 'True Color (432)');
print(image)
//median (ndvi)
var ndvi = image.normalizedDifference(['SR_B5','SR_B4']).rename('NDVI');
var ndviparams = {min: -1, max: 1, palette: ['blue', 'white', 'green']};
print(ndvi, 'ndvi');
Map.addLayer(ndvi, ndviparams, 'ndvi');
}
//select thermal band10(with brightness temperature)
var thermal= image.select('ST_B10').multiply(0.1);
var b10params = {min: 291.918, max:302.382, pallete:['blue', 'white', 'green']};
Map.addLayer(thermal, b10params, 'thermal');
//find the min and max of NDVI
{
var min = ee.Number(ndvi.reduceRegion({
reducer: ee.Reducer.min(),
scale: 30,
```

```
maxPixels: 1e9
}).values().get(0));
print(min, 'min');
var max = ee.Number(ndvi.reduceRegion({
reducer: ee.Reducer.max(),
scale: 30,
maxPixels:1e9
}).values().get(0));
print(max, 'max')
}
//fractional vegetation
{
var fv =(ndvi.subtract(min).divide(max.subtract(min))).pow(ee.Number(2))
print(fv, 'fv');
Map.addLayer(fv);
}
//Emissivity
var a= ee.Number(0.004);
var b= ee.Number(0.986);
var EM=fv.multiply(a).add(b).rename('EMM');
var imageVisParam3 = {min: 0.9865619146722164, max: 0.98699971371314};
Map.addLayer(EM, imageVisParam3, 'EMM');
//LST in Celsuis Degree bring c
//NB: In Kelvin don't bring -273.15
var LST = thermal.expression(
'(Tp/(1+(0.00115* (Tp/ 1.438))*log(Ep)))', {
'Tp': thermal.select('ST_B10'),
'Ep': EM.select('EMM')
}).rename('LST');
//min max LST
var min = ee .Number(LST.reduceRegion({
reducer: ee.Reducer.min(),
scale: 30,
maxPixels: 1e9
}).values().get(0));
print(min, 'minLST');
var max = ee .Number(LST.reduceRegion({
reducer: ee.Reducer.max(),
scale: 30,
maxPixels: 1e9
}).values().get(0));
print(max, 'maxLST');
```

Figure 6: Shows the GEE code for calculating the land surface temperature.

4. Results and Discussion

Landsat multispectral bands were used to investigate the spectral responses of built-up areas, vegetative cover, and watersheds. All three types had a distinct signature in optical bands, indicating they could be distinguished from their relevant indicators. The overall spatial distribution of vegetative cover, watersheds, and built-up areas was calculated using Google Earth Engine (GEE) data and the NDVI, NDWI, and NDBI indices. The GEE provides colossal capabilities for dealing with large volumes of remote sensing imagery and a collection of classification methodologies used for spatial analysis via JavaScript APIs. The results revealed that the urbanized areas increased dramatically after 2004, while the vegetative cover and greenery spaces declined. On the other hand, the watersheds fluctuated between increased and decreased during the study period, see Table 1.

Table 1: The results of indices calculation over Baghdad during the study period.

Years	Vegetative coverage (Km^2)	Urbanized areas (km^2)	Watersheds (km^2)	Open lands (km^2)
2004	3476	835	51	743
2008	2460	1690	41	869
2013	2242	1820	67	1067
2017	1522	2625	79	920
2021	1368	2694	80	906

The urbanized areas expanded by 1859.0 km^2 from 835.0 to 2694.0 km^2 during 2004-2021; vegetative cover decreased by 2108.0 km^2 from 3476.0 to 1368.0 km^2 during 2004-2021, Figures 7 and 8.

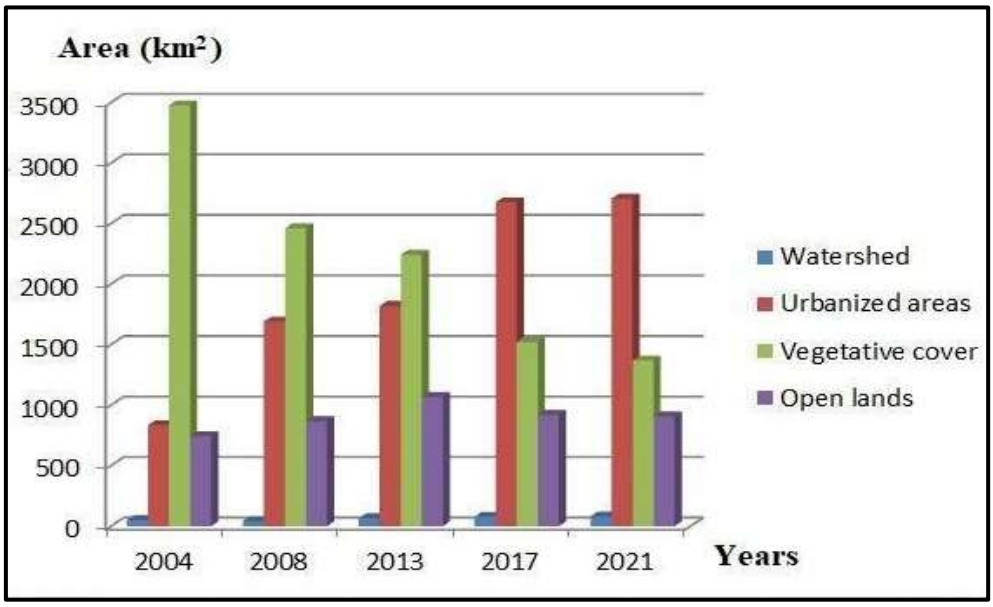

Figure 7: The graphical representation of Landsat analysis according to the land cover indices.

The watershed amount depends on factors like rainfall in Iraq and upstream countries, the water share from upstream countries, and the differences between seasons. The open lands also have subjected an increase of about 163.0 km^2 in Baghdad throughout the study period. This category contained barren lands, salty lands, fertile and uncultivated soil, and former military. Figure 8 represents the land cover changes in Baghdad and the distribution of the categories above, which were calculated according to the land cover indices using the GEE service.

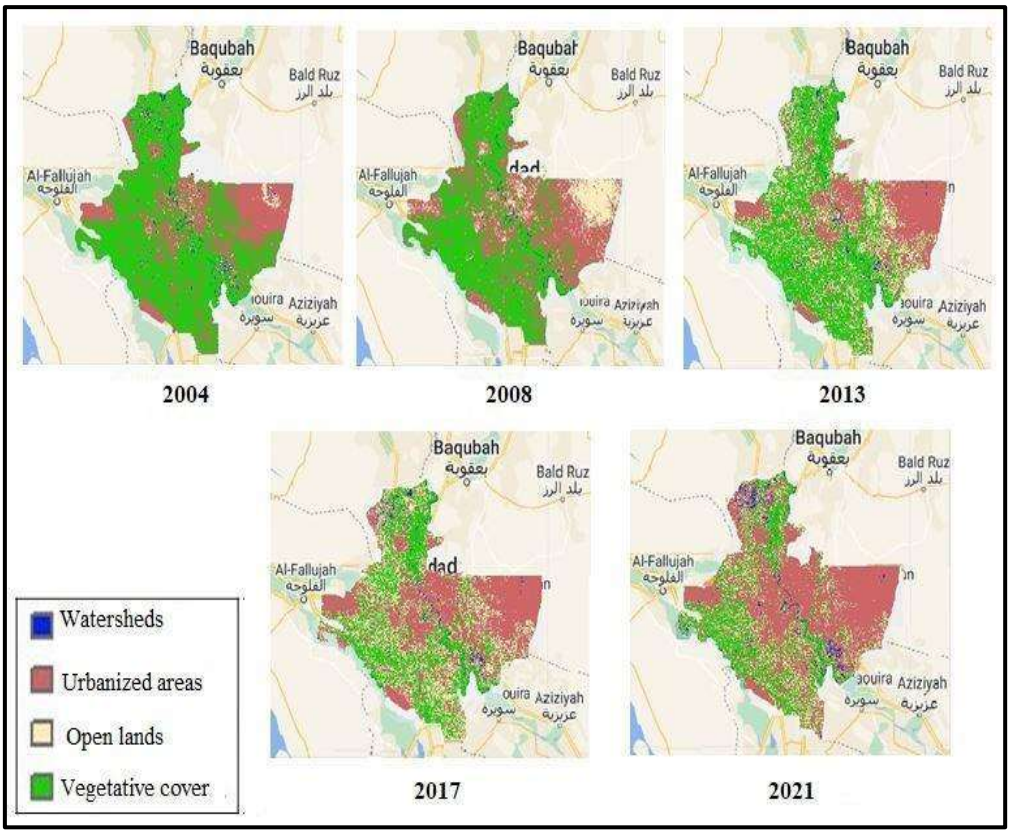

Figure 8: The expansion of urbanized and open land and the degradation of the vegetative areas.

Figure 9 demonstrates the difference between the distribution of the four land cover categories over Baghdad during the last 17 years. The vegetative cover declined from 68% to 27% during 2004-2021, while the urbanized areas increased from 16% to 53% during 2004-2021. In contrast, the category of open land decreased from 18% to 15% during 2004-2021, but the open land areas increased, indicating the possibility of transforming a part of the vegetative cover to open land. At the same time, this case also applies to the watershed, where its percentage increased, although it depends on several factors and fluctuates from year to year.

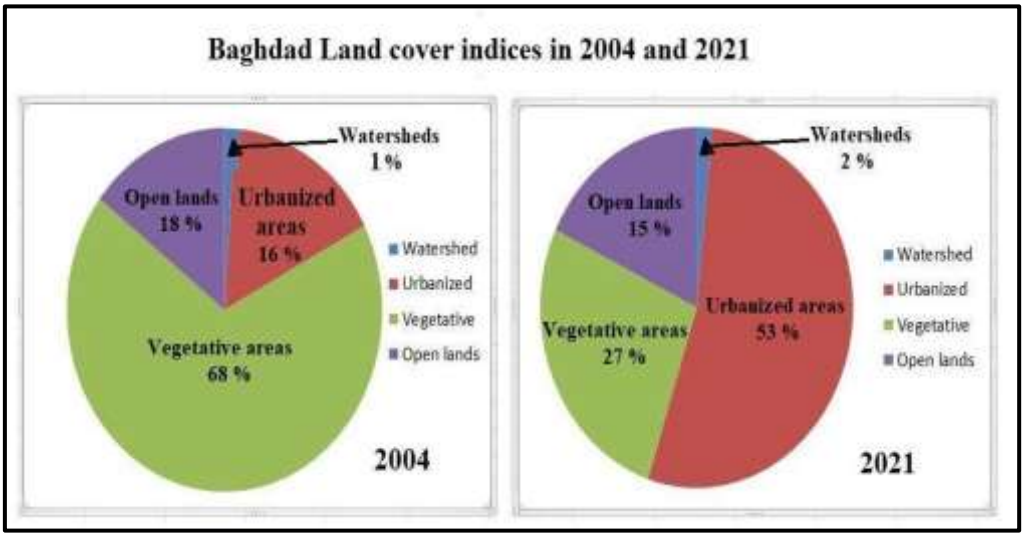

Figure 9: The difference in land cover in Baghdad between 2004 and 2021.

On the other hand, the noticeable land cover change led to studying this change's impacts on Baghdad's climate warming. Hence, the land surface temperature in Baghdad using Landsat 5 for 2004 and Landsat 8/TOA for 2021 has also been calculated.

As GEE offers satellite images freely, the land surface temperature was determined directly using the codes shown in Figure 6. The findings revealed that the minimum temperature in Baghdad was 44° C in 2004 and has increased to 46.5° C in 2021. Moreover, the maximum temperature was 56° C in 2004 and rose to 60° C in 2021.

Figure 10 shows the land surface temperature (LST) gradient according to the land cover type. The blue color in Figure 10 shows the minimum surface temperature, which is concentrated along the watersheds. It extends from the northeast to the southeast of Baghdad city along the Tigris River. The green and yellow colors indicate hotter areas than watersheds, while the red represents the hottest areas. The maximum land temperature is concentrated on open lands and urbanized areas, as shown in the comparison between the land cover thematic maps derived by indices (Figure 9) and the maps showing the distribution of land surface temperature (Figure 10). Therefore, vegetation and watersheds have a more significant influence on the land surface temperature due to their cooler impact

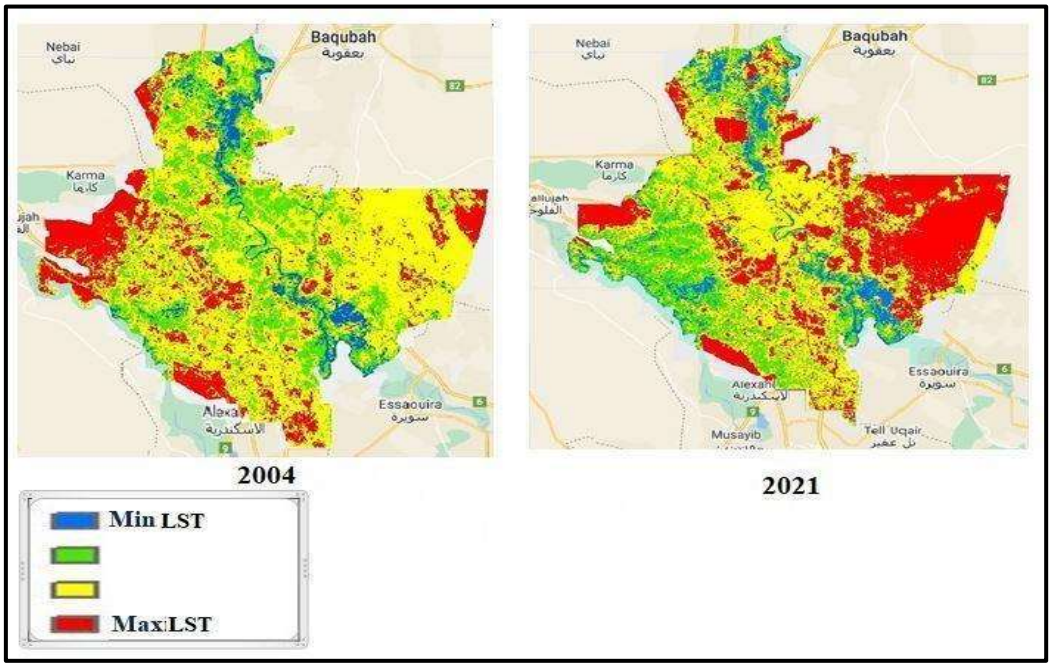

Figure 10: The distribution of land surface temperature (LST) over Baghdad.

5. Discussion and Conclusion

The main objective of this study was to analyze and examine the local climate warming in Baghdad city and produce an automated thematic map using the GEE service. Baghdad's inhabitance has grown significantly due to social, political, and security factors, educational needs, business demands, medical treatment, and the availability of basic infrastructure and services. As a result, Baghdad city increasingly crowded over time. Hence, large residential, commercial, and industrial areas would be developed, and large residential, commercial, and industrial areas would be developed to accommodate the inhabitance growth and meet essential needs. This study focused on addressing the problem of the side effect of unplanned urbanization areas, which spread after 2004, to investigate the land cover/ land use change and the distribution of greenery areas.

The GEE plays a vital role in determining the areas of the land cover and creating thematic maps to reveal their distribution using land cover indices such as NDVI, NDWI, and NDBI. The findings showed that the urbanized areas in 2004 were 16% and increased by 53% in 2021. The open land increased by 3% during the study period, while the vegetative cover decreased from 68% in 2004 to 27% in 2021.

The maximum land surface temperature has risen by 3°C between 2004 and 2021, while the minimum land surface temperature has risen 2°C over Baghdad during the same period. This can submit an alarming fact that unplanned urbanized transformation that causes the degradation of vegetative cover and greenery land is one of the most important causes of regional warming and air pollution, resulting in the Urban Heat Island (UHI) effect. It is essential to try to reduce this phenomenon and focus on efforts to find convenient solutions to mitigate its effects on local and global warming.

References

[1] L. Koschke, C. Furst, S. Frank and F. Makeschin, "A multi-criteria approach for an integrated land-cover-based assessment of ecosystem services provision to support landscape planning," *Ecological indicators*, vol. 21, pp. 54-66, Oct. 2012.

[2] S. Niquisse, P. Cabral, A. Rodrigues, and G. Augusto, "Ecosystem services and biodiversity trends in Mozambique as a consequence of land cover change," *International Journal of Biodiversity Science, Ecosystem Services & Management,* vol. 13, no. 1, pp. 297-311, Jun. 2017.

[3] R. Kamel and S. N. Jasim, "Improving of Green Cover and Exterior Landscape Design of Baghdad University ' Jadriyah Campus," *Iraqi J. Agric. Sci.*, vol. 48, no. 6, Nov. 2017.

[4] T. N. Phan, V. Kuch, & L. W. Lehnert, "Land Cover Classification using Google Earth Engine and Random Forest Classifier—The Role of Image Composition," *Remote Sensing*, *12*(15), 2411, (2020).

[5] T. Chikowore and L. Willemse, "Identifying the changes in the quality of life of Southern African Development Community (SADC) migrants in South Africa from 2001 to 2011," *South African Geographical Journal (Suid-Afrikaanse Geografiese Tydskrif*, Jan. 2017 [Online]. Available: hdl.handle.net/10520/EJC198152.

[6] A. K. M. . Ali and F. K. M. . Al Ramahi, "A study of the Effect of Urbanization on Annual Evaporation Rates in Baghdad City Using Remote Sensing," *Iraqi Journal of Science*, vol. 61, no. 8, pp. 2142–2149, Aug. 2020.

[7] R. R. Al-Ani, A.-A. J. Al-Obaidy and F. M. Hassan, "Multivariate Analysis for Evaluation The Water Quality of Tigris River within Baghdad City in Iraq," *Iraqi Journal of Agricultural Sciences*, vol. 50, p. 1, 2019.

[8] A. A.-R. Sadiq, "Convolution," *Journal of Physics: Conference Series*, vol. 1530, May 2020

[9] K. Fahad, H. Sabah, and H. Dibs, "Spatial-temporal analysis of land use and land cover change detection using remote sensing and GIS techniques." In *IOP Conference Series: Materials Science and Engineering*, vol. 671, 2020, doi: 10.1088/1757-899X/671/1/012046.

[10] M. Khine, Y. Maw, and M. Win, "Change analysis of indices (NDWI, NDVI, NDBI) for Mawlamyine City area using google earth engine.," *J. Myanmar Acad. Arts Sci*, 2018.

[11] H. A. Zurqani, C. J. Post, E. A. Mikhailova, & J. S. Allen, "Mapping urbanization trends in a forested landscape using Google Earth Engine," *Remote Sensing in Earth Systems Sciences*, vol. *2*, no. 4, pp. 173-182,2019.

[12] O. Mutanga, & L. Kumar, "Google earth engine applications," *Remote Sensing*, vol. 11, no. 5, p.591, 2019.

[13] J. Weier, & D. Herring, "Measuring vegetation (ndvi & evi)," *NASA Earth Observatory*, *20*, 2, 2000.

[14] S. K. McFeeters, "The use of the Normalized Difference Water Index (NDWI) in the delineation of open water features," *International Journal of Remote Sensing*, vol. 17, no.7, pp. 1425–1432, 1996.